NASA/TM—2016-219076 AIAA–2016–1647

# Impact of an Exhaust Throat on Semi-Idealized Rotating Detonation Engine Performance

*Daniel E. Paxson*
*Glenn Research Center, Cleveland, Ohio*

April 2016

# NASA STI Program . . . in Profile

Since its founding, NASA has been dedicated to the advancement of aeronautics and space science. The NASA Scientific and Technical Information (STI) Program plays a key part in helping NASA maintain this important role.

The NASA STI Program operates under the auspices of the Agency Chief Information Officer. It collects, organizes, provides for archiving, and disseminates NASA's STI. The NASA STI Program provides access to the NASA Technical Report Server—Registered (NTRS Reg) and NASA Technical Report Server—Public (NTRS) thus providing one of the largest collections of aeronautical and space science STI in the world. Results are published in both non-NASA channels and by NASA in the NASA STI Report Series, which includes the following report types:

- TECHNICAL PUBLICATION. Reports of completed research or a major significant phase of research that present the results of NASA programs and include extensive data or theoretical analysis. Includes compilations of significant scientific and technical data and information deemed to be of continuing reference value. NASA counter-part of peer-reviewed formal professional papers, but has less stringent limitations on manuscript length and extent of graphic presentations.

- TECHNICAL MEMORANDUM. Scientific and technical findings that are preliminary or of specialized interest, e.g., "quick-release" reports, working papers, and bibliographies that contain minimal annotation. Does not contain extensive analysis.

- CONTRACTOR REPORT. Scientific and technical findings by NASA-sponsored contractors and grantees.

- CONFERENCE PUBLICATION. Collected papers from scientific and technical conferences, symposia, seminars, or other meetings sponsored or co-sponsored by NASA.

- SPECIAL PUBLICATION. Scientific, technical, or historical information from NASA programs, projects, and missions, often concerned with subjects having substantial public interest.

- TECHNICAL TRANSLATION. English-language translations of foreign scientific and technical material pertinent to NASA's mission.

For more information about the NASA STI program, see the following:

- Access the NASA STI program home page at http://www.sti.nasa.gov

- E-mail your question to help@sti.nasa.gov

- Fax your question to the NASA STI Information Desk at 757-864-6500

- Telephone the NASA STI Information Desk at 757-864-9658

- Write to:
  NASA STI Program
  Mail Stop 148
  NASA Langley Research Center
  Hampton, VA 23681-2199

NASA/TM—2016-219076 AIAA–2016–1647

# Impact of an Exhaust Throat on Semi-Idealized Rotating Detonation Engine Performance

*Daniel E. Paxson*
*Glenn Research Center, Cleveland, Ohio*

Prepared for the
Scitech 2016
sponsored by the American Institute of Aeronautics and Astronautics
San Diego, California, January 4–8, 2016

National Aeronautics and
Space Administration

Glenn Research Center
Cleveland, Ohio 44135

April 2016

This report is a formal draft or working paper, intended to solicit comments and ideas from a technical peer group.

This report contains preliminary findings, subject to revision as analysis proceeds.

*Level of Review*: This material has been technically reviewed by technical management.

Available from

NASA STI Program
Mail Stop 148
NASA Langley Research Center
Hampton, VA 23681-2199

National Technical Information Service
5285 Port Royal Road
Springfield, VA 22161
703-605-6000

This report is available in electronic form at http://www.sti.nasa.gov/ and http://ntrs.nasa.gov/

# Impact of an Exhaust Throat on Semi-Idealized Rotating Detonation Engine Performance

Daniel E. Paxson
National Aeronautics and Space Administration
Glenn Research Center
Cleveland, Ohio 44135

## Abstract

A computational fluid dynamic (CFD) model of a rotating detonation engine (RDE) is used to examine the impact of an exhaust throat (i.e., a constriction) on performance. The model simulates an RDE which is premixed, adiabatic, inviscid, and which contains an inlet valve that prevents backflow from the high pressure region directly behind the rotating detonation. Performance is assessed in terms of ideal net specific impulse which is computed on the assumption of lossless expansion of the working fluid to the ambient pressure through a notional diverging nozzle section downstream of the throat. Such a semi-idealized analysis, while not real-world, allows the effect of the throat to be examined in isolation from, rather than coupled to (as it actually is) various loss mechanisms. For the single Mach 1.4 flight condition considered, it is found that the addition of a throat can yield a 9.4 percent increase in specific impulse. However, it is also found that when the exit throat restriction gets too small, an unstable type of operation ensues which eventually leads to the detonation failing. This behavior is found to be somewhat mitigated by the addition of an RDE inlet restriction across which there is an aerodynamic loss. Remarkably, this loss is overcome by the benefits of the further exhaust restrictions allowed. The end result is a configuration with a 10.3 percent improvement in ideal net specific thrust.

## Nomenclature

| | |
|---|---|
| $A_{annulus}$ | annulus area |
| $A_{exit}$ | exit area |
| $A_{in}$ | inlet area |
| $a^*$ | reference speed of sound, 1250 ft/sec |
| $\gamma$ | ratio of specific heats |
| $I_{nspi}$ | ideal net specific impulse |
| $I_{anspi}$ | algebraically computed ideal net specific impulse |
| $P$ | non-dimensional total pressure |
| $p$ | non-dimensional static pressure |
| $P_{man}$ | non-dimensional RDE inlet manifold total pressure |
| $p^*$ | reference pressure, 14.7 psia |
| $R_g$ | real gas constant |
| $\rho$ | non-dimensional density |
| $s$ | non-dimensional entropy |
| $T$ | non-dimensional static temperature |
| $T_t$ | non-dimensional total temperature |
| $T_{man}$ | non-dimensional RDE inlet manifold total temperature |
| $T^*$ | reference temperature, 520 °R |
| $t$ | non-dimensional time |

$u$ non-dimensional circumferential velocity
$u_{det}$ non-dimensional circumferential detonation velocity
$v$ non-dimensional axial velocity
$x$ non-dimensional circumferential distance
$y$ non-dimensional axial distance

# I. Introduction

The rotating detonation engine (RDE) is under investigation as an approach to pressure gain combustion (PGC) for propulsion and power systems. In its basic form, the RDE essentially consists of an annulus with one end open and the other end valved (mechanically, or aerodynamically). Fuel and oxidizer enter axially through the valved end. The detonation travels circumferentially. Combustion products exit predominantly axially through the open end. The majority of the fluid entering the device is passed over or 'processed' by the rotating detonation wave which substantially raises the pressure and temperature. As the fluid continues to move, it is expanded and accelerated through the exhaust end, thereby producing thrust. An example of a basic RDE cycle can be seen in Figure 1, which shows computed contours of temperature throughout the 'unwrapped' annular region. The figure shows data in the detonation frame of reference which, for the code used, makes it invariant in time (Ref. 1). Also shown in the figure are profiles of non-dimensionalized (i.e., normalized by reference values) total pressure and axial velocity at the inlet and exhaust planes, as well as select streamlines. The computed result represents a stoichiometrically fueled hydrogen/air RDE. In a ram propulsion application, the inlet and exit conditions correspond to a Mach = 1.37 flight condition, at 37,000 ft, using Mil. Spec. pressure recovery (Ref. 2). The ideal net specific impulse is $I_{nspi}$ = 3846 sec. This was obtained by computing the ideally expanded specific thrust from each fluid element in the RDE exit plane and then performing a mass average (Ref. 3). Such a calculation provides an estimate (admittedly optimistic) of performance without having to add, and compute the flowfield of, an exit nozzle. It is noted from the inlet flow

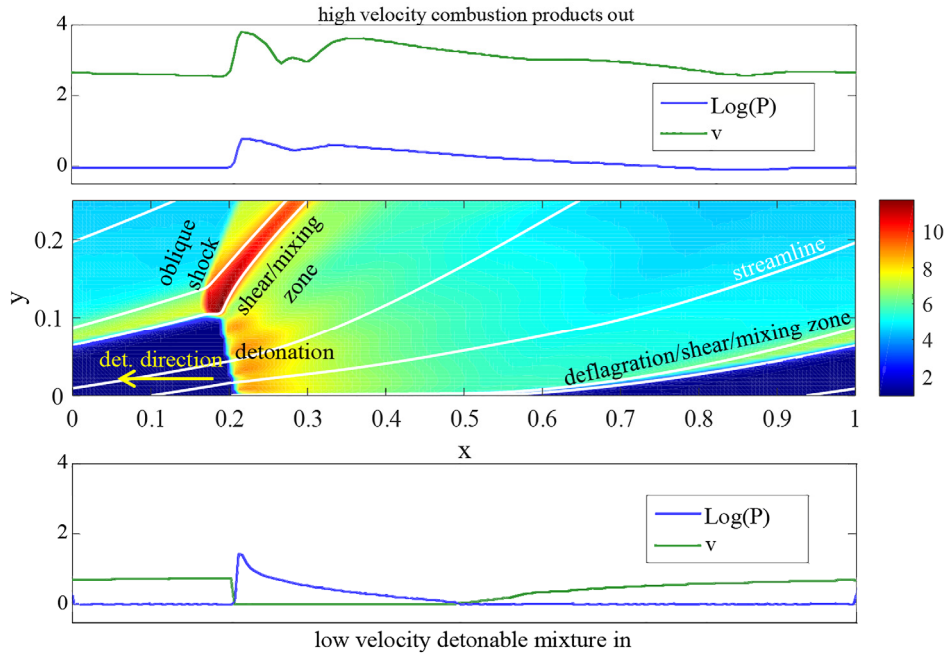


Figure 1.—Computed contours of non-dimensional temperature throughout the annulus of an 'unwrapped' idealized RDE, in the detonation frame of reference. The RDE is operating on premixed, stoichiometric $H_2$ and Air.

distribution shown in Figure 1 that the RDE under consideration is idealized in having a perfect valve system that does not permit backflow, and which, for this example, is lossless. Additionally, as will be briefly detailed in the code description section of the paper, the RDE is assumed adiabatic and the working fluid is inviscid, premixed, and calorically perfect. It is noted here that throughout this paper, unless explicitly stated, all fluid properties are non-dimensionalized or normalized with respect to reference values. Velocities are normalized by the reference speed of sound. Lengths are normalized by the RDE circumference, and time is normalized by the ratio of circumference to the reference speed of sound. The reference values are listed in the nomenclature section.

The computed ideal net specific impulse is approximately 21 percent higher than would be obtained by an ideal conventional ramjet (i.e., constant pressure combustion) under the same assumptions; however, it is 22 percent lower than would be predicted from an algebraic analysis of a purely one-dimensional (1D) detonative PGC cycle as has been done with pulsed detonation engines (PDE's) (Ref. 4). Approximately 6 percent of the latter 22 percent disparity comes from the fact that algebraic analysis methods do not account for the unavoidable impact of exit flow non-uniformity (Ref. 3). The 6 percent value was obtained using the time-accurate, CFD-based PDE model described in Reference 5 to compute the idealized specific impulse of a PDE under the flight conditions described in this paper and comparing it to the algebraic model also described in Reference 5. Another approximately 5 percent can be accounted for by the fact that some of the chemical energy in an RDE is converted into circumferential kinetic energy, which does not contribute to thrust (Ref. 1). There are other minor contributions to ideal RDE/PDE performance disparity such as the inevitable deflagration region of the RDE, the associated shear layer, and the oblique shock that are not present in the ideal PDE. These are seen in Figure 1, and are highlighted in Figure 2, which shows contours of entropy relative to the entropy found at the Chapman-Jouguet (C-J) point of a purely 1D detonation (e.g., in a PDE) under the same idealizations as used to compute the RDE flowfield (Ref. 6). Entropy is normalized using the mixture gas constant. Fluid at a lower entropy than the C-J point is not included in Figure 2 and is shown as a white region. Increased entropy results in decreased availability of the fluid for producing thrust. While the entropy in the vicinity of the above mentioned flow structures is indeed well above the C-J point, it only involves 26 percent of the flow passing through the RDE. It is possible to mass-average the entropy of the Figure 2 exit flow and use it, along with the known mass-averaged total temperature to crudely estimate an ideal specific impulse (Ref. 5).

For reference, the mass-average of any quantity, $f$, at a plane is defined as follows.

$$\bar{f} = \frac{\int (\rho u f)dy}{\int (\rho u)dy} \tag{1}$$

The mass-averaged Figure 2 exit entropy can also be calculated with the high entropy region excluded, and a similar specific thrust estimate can also be made. The difference between them represents a rough estimate of the impact of these so-called 'minor' losses, which accounts for another 4 percent of the 22 percent ideal RDE/algebraic PDE disparity.

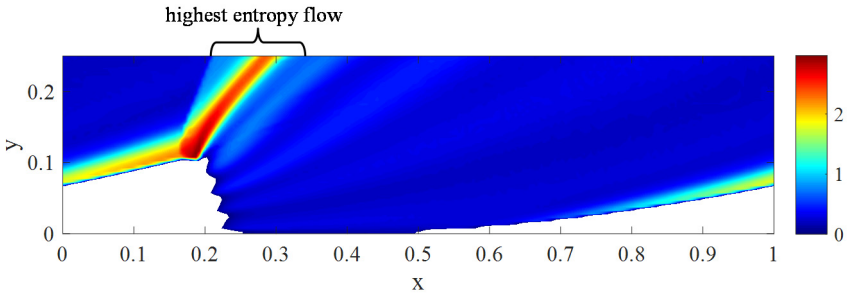


Figure 2.—Computed contours of entropy relative to C-J entropy throughout the annulus of the Figure 1 RDE. Only positive relative entropy is shown.

This leaves a remaining 7 to 10 percent disparity which is the subject of this paper. The entire blue region of Figure 2 (i.e., fluid with entropy above that of the 1D CJ point) can be attributed to entropy produced by the rotating detonation itself. This entropy is greater than the idealized 1D detonation process because the latter assumes a negligible fill Mach number (i.e., the Mach number of the unreacted fluid filling the RDE and through which the detonation propagates), while the basic RDE shown here has a relatively high value. The impact of fill Mach number on performance will be described, and an approach to controlling it, and thereby mitigating its impact will then be presented. That approach is the addition of an exhaust restriction or throat. It will be shown that, in this idealized simulation environment, an approximately 10 percent net specific thrust improvement over the basic RDE configuration of Figure 1 can be achieved. The improvement is not without complications however, due to the highly coupled nature of RDE operation. These complications will be detailed. Since the entire investigation utilizes a particular CFD-based RDE model, a brief description of it will precede all else. More details of the model and validation results may be found in References 1, 7, and 8.

# II. Model Description

The model basis is a high resolution, computational fluid dynamic (CFD) algorithm that integrates the quasi-two-dimensional, single-species, reactive Euler equations with source terms. The code adopts the detonation frame of reference and deliberately utilizes a course grid (i.e., is diffusive) in order to eliminate the highest frequency unsteadiness (e.g., detonation cells, Kelvin-Helmholtz phenomena). All of the results shown in this paper utilize only 10,000 grid points. The result is a flowfield solution that is invariant with time when converged. As mentioned earlier, the working fluid is assumed to be a single, calorically perfect, premixed gas. Relevant properties used in all calculations of this paper are a real gas constant, $R_g$, of 73.92 ft-$lb_f$/$lb_m$/R, and a ratio of specific heats, $\gamma$, of 1.264 (Refs. 5 and 7).

The source terms contain sub-models which govern the reaction rate, momentum losses due to skin-friction, and the effects of heat transfer to the walls. The sub-models are adapted from validated one-dimensional sub-models used to investigate pulse detonation engines and other gasdynamic devices (Refs. 9 to 11). For the present idealized study, only the reaction rate sub-model will be used. Due to the simplicity of this sub-model two reaction rate constants are required: a large one for regions of detonation and a smaller one for regions of deflagration as shown in Figure 1. Based on past validation efforts with experiments (Refs. 7 and 8), the deflagrative rate constant is set to a value such that, in combination with other fluid dynamic processes, approximately 6 percent of the premixed RDE throughflow reacts in this region. The remaining 94 percent detonates.

The governing equations are integrated numerically in time using an explicit, second-order, two-step, Runge-Kutta technique. Spatial flux derivatives are approximated as flux differences, with the fluxes at the discrete cell faces evaluated using Roe's approximate Riemann solver. Second-order spatial accuracy (away from discontinuities) is obtained using a so-called MUSCL technique (i.e., Monotonic Upstream-Centered Scheme for Conservation Laws) whereby the primitive variable states within the cells are represented as piecewise linear rather than constant as first order accuracy would imply. Oscillatory behavior is avoided by limiting the linear slopes.

Considering the Figure 1 RDE where the non-dimensional circumferential direction is $x$, and the axial direction is $y$, the following boundary conditions are imposed. At $x = 0.0$ and $x = 1.0$, periodic (aka symmetric) conditions are used. These ensure that the x-dimension of the computational space faithfully represents an annulus (which is continuous and has no boundary). At $y = y_{max}$, constant pressure outflow is imposed along with characteristic equations to obtain $\rho$ and $v$ for the image cells. If the resulting flow is sonic, or supersonic, then the imposed pressure is disregarded. If, in addition, the upstream flow is supersonic, then $p$, $\rho$, and $v$ are extrapolated from the interior (Ref. 12). The possibility for a normal shock solution whereby supersonic outflow jumps to subsonic is also accommodated. The x-velocity component $u$ is extrapolated from the interior at each boundary location. At $y = 0.0$ (the inflow face), partially open boundary conditions are applied as described and validated in Reference 13. This face is

presumably fed by a large manifold at a fixed total pressure, and temperature. The manifold terminates at the face and is separated from it via an orifice. The ratio of orifice flow area to RDE annulus area, ε, is generally less than 1. If the interior pressure is less than the manifold pressure, $P_{man}$, then inflow occurs. The boundary condition routine determines $p$, ρ, and $v$ for the inflow face image cells subject to a momentum (total pressure) loss model which depends on the mass flow rate and the value of ε. The routine is capable of accommodating a scenario where the inflow becomes choked. For most (but not all) of this investigation, ε is assigned a value of 1, which ensures a lossless inlet. The x-velocity component $u$ is prescribed during inflow, and it is here that a reference frame change is implemented. Rather than specify $u = 0$ (i.e., no swirl) which is the laboratory or fixed frame condition, the negative of the detonation speed, $u_{det}$ is prescribed instead. As a result of this change to the detonation reference frame, the computational space becomes one where a steady-state solution is possible. If the interior pressure along the inlet face is greater than $P_{man}$, as might be found just behind the detonation, then there will be backflow into the manifold through the orifice. The boundary condition routine can accommodate this as well. However, for this investigation a notional check-valve boundary condition is implemented which detects when backflow would normally occur, and applies a solid wall boundary condition.

### A. Exit Throat

The exit throat to be used for control of fill Mach number could have been implemented using the quasi-two-dimensional capability of the code. That is, a converging profile of the annulus width could have been prescribed near the exhaust end of the RDE. Instead however, a partially open outflow boundary condition was imposed (Ref. 13). The boundary condition method assumes that the axial extent of the throat is negligible, and that the flow within the negligibly small region is isentropic. It has the advantage of being convenient for parametric variations of the throat area over a wide range because the throat size can be specified as a single input parameter to the model.

## III. Effects of Fill Mach Number

The relationships between entropy (relative to the combustor inlet), ideal net specific thrust, and fill Mach number can be calculated algebraically for an idealized, 1D detonation (Refs. 4 and 6) under the assumptions of the Figure 1 operating point. These are shown in Figure 3. It can be seen that as the fill

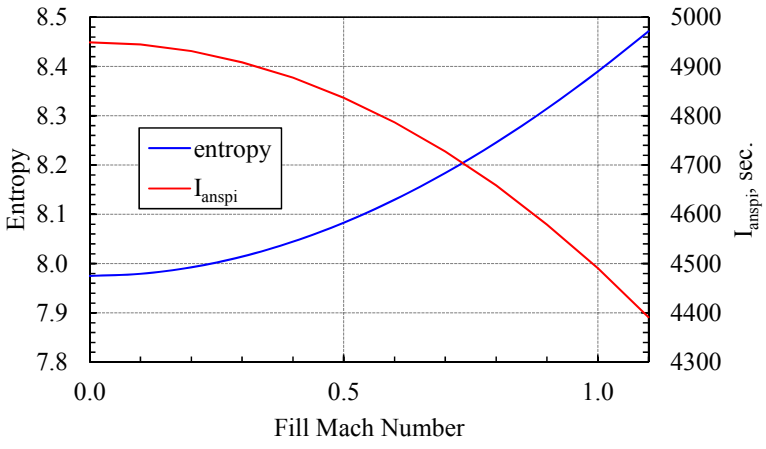


Figure 3.—Analytically determined entropy and algebraic ideal net specific thrust as functions of fill Mach number for an ideal 1D detonation device such as a PDE.

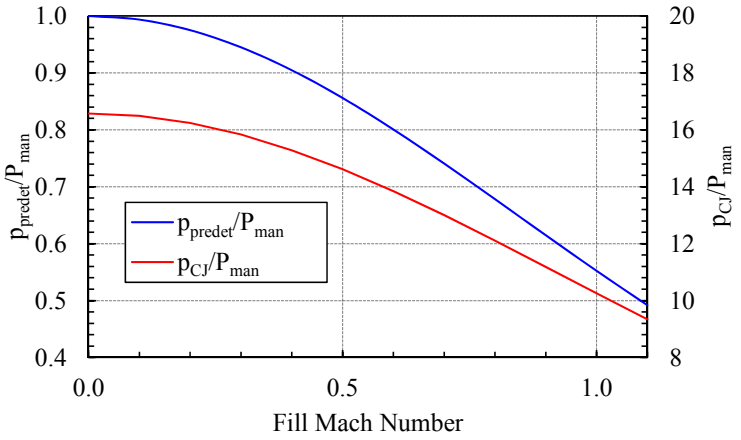


Figure 4.—Analytically determined pre- and post-detonation (i.e., CJ) pressures as functions of fill Mach number for an ideal 1D detonation device such as a PDE.

Mach number rises, the entropy generated in the detonation rises and the specific impulse drops. A somewhat heuristic explanation for this trend is shown in Figure 4. Here the static pressures just prior to and just after the detonation event are plotted as functions of the fill Mach number. Both have been normalized by the manifold total pressure just upstream of the notional device in which the 1D detonation is taking place. As the fill Mach number increases, the pre-detonation pressure drops as dictated by isentropic relationships for accelerating flows. Being isentropic, there is no availability loss (i.e., ability of the flow to do work) associated with this pressure drop. The flow is simply exchanging potential for kinetic energy. However, the deto process has no mechanism to utilize the kinetic energy, and there is no pressure recovery preceding the propagation of the detonation through the accelerated flow. As such, the 1D detonation produces a smaller pressure ratio relative to the manifold total pressure as the fill Mach number increases. This leads to higher entropy and reduced availability. While this is a simplified explanation, and while an RDE does not produce a one-dimensional detonation, it does provide a theoretical estimate for the magnitude of the effect.

The relationship between fill Mach number and performance is more difficult to demonstrate in a RDE simulation; however, an attempt is made in Figure 5, which shows two quantities as functions of the axial distance, y. Referring to Figure 1, the blue curve represents axial Mach number at x = 0.19 which is just prior to the fluid entering the detonation front (in this frame of reference). This may be considered the RDE equivalent of the pre-detonative fill Mach number. The axial extent of the line represents the region where all of the fluid has zero entropy. Passing through this region is 78 percent of the total inflow. The green curve represents entropy (relative to a value of 8) at x = 0.29, which is the point where all reactions have ceased (i.e., post-detonation). The axial extent of this curve was selected such that it has the same mass flow across it as the pre-detonation curve. The somewhat “wavy” nature of this curve is the result of coarseness in the computational grid. It does not affect performance or overall trend. The difference between pre- and post-detonative axial extent (for the same mass flow) is caused by fluid expansion in the axial direction. For reference, the planes described above are shown as vertical dashed lines in the inset to Figure 5, which is actually a sub-region of Figure 1. If the Mach number is fit linearly to the axial distance normalized by the maximum axial value shown, and the same is done for the entropy, then normalized axial value can be eliminated between the two fits, resulting in a crude estimate relating fill Mach number to post-detonative entropy. Alternately, the mass-averaged Mach number and entropy can be calculated for all computational points along the blue and green lines of Figure 5, respectively. Both of these estimates are shown in Figure 6, which also repeats the Figure 3 analytical 1D Mach number versus entropy line. It is seen that the relationship between fill Mach and entropy (and by extension availability) for an RDE is much the same as a PDE.

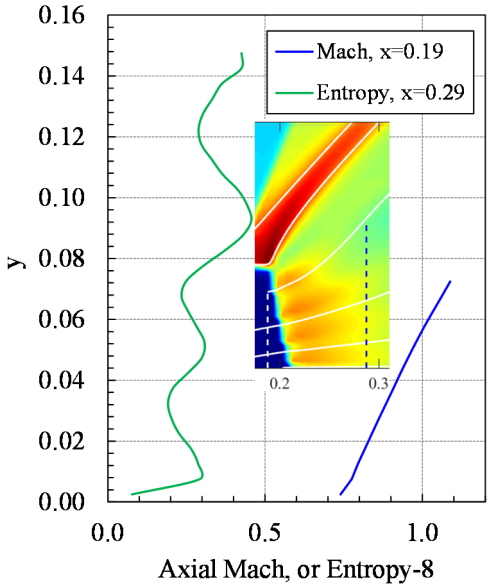


Figure 5.—Pre-detonative axial Mach number and post-detonative entropy as functions of axial distance in the Figure 1 flowfield.

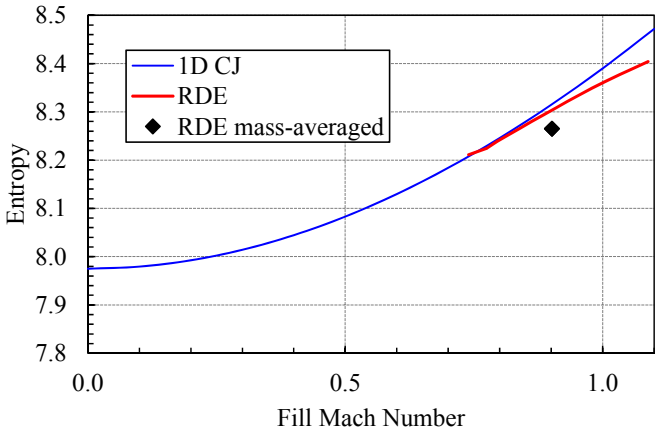


Figure 6.—Estimated and mass-averaged RDE entropy, and algebraic ideal 1D detonation entropy as functions of fill Mach number.

## IV. Fill Mach Control

The need to control the fill Mach number has long been recognized in PDE's, particularly in scenarios where the exit static pressure is substantially below the inlet total pressure (e.g., high speed flight) (Ref. 14). The most common approach is to add a constriction, or throat at the exhaust end which, by slowing the expansion rate, also slows the fill rate and maintains a relatively high predetonative pressure. Of course, such an approach can reduce the flow rate through the device. As such, it may necessitate a larger device for a given application. Additionally, an exit throat provides a reflective surface for the incident detonation wave. This results in shock waves traveling back upstream and in some circumstances impacting the subsequent fill process (Ref. 15). Still, an exhaust throat is effective in PDE's and is the approach used in the present investigation for RDE's.

# V. Results

The simulation was run to convergence for the exact same conditions and configuration as Figure 1 except the ratio of exit to annulus area was incrementally reduced from a value of 1.0. The increment was –0.05 (i.e., $A_{exit}/A_{annulus}$ = 0.95, 0.90, 0.85, etc.). With each incremental reduction the specific impulse improved. Figure 7 shows contours of temperature and pressure (actually the Log of pressure due to the immense pressure variations observed) for the case where $A_{exit}/A_{annulus}$ = 0.75. This value represents a limit for reasons to be described below in Subsection A. It can be seen immediately that the flowfield has changed substantially. Axial velocities have been reduced as evidenced by the lower detonation height, and the 'bending back' of the shear/mixing zone relative to Figure 1. Gasdynamic waves are seen to reflect from the throat and travel upstream where they mildly impinge on the inlet. They also provide the benefit in this case of slightly compressing a portion of the incoming flow. The entropy-averaged total pressure, $P_{EA}$, just to the left of the detonation front (i.e., x = 0.19, 0<y<0.053) is 11 percent above the inlet manifold total pressure. As discussed in Reference 15, entropy-averaging is a technique for obtaining a meaningful, single value for total pressure which represents an entire region of the flowfield (a plane in this case). It is the total pressure, at the mass-averaged total temperature crossing the plane of interest, which produces the mass-averaged entropy crossing the plane of interest. It is calculated using the following equation.

$$P_{EA} = P_{man}\left(\frac{\bar{T}_t}{T_{man}}\right)^{\frac{\gamma}{\gamma-1}} e^{-\bar{s}} \tag{2}$$

The average axial Mach number in this region has dropped from 0.90 to 0.53. The mass-averaged post-detonation entropy has dropped from 8.27 to 7.92 (Fig. 6). This is just 2 percent below the entropy predicted by the 1D CJ relationship (Fig. 6), further indicating that the same mechanisms are at work in the RDE as in the PDE. Not surprisingly, the ideal net specific impulse increases by 9.4 percent to 4209 sec. Interestingly too, the mass flow rate actually increases by approximately 2.6 percent with the exit throat in place. The reason for this is not clear since it is difficult to decouple all of the processes occurring in the RDE cycle. However, one reasonable mechanism may be as follows. The exit flows of

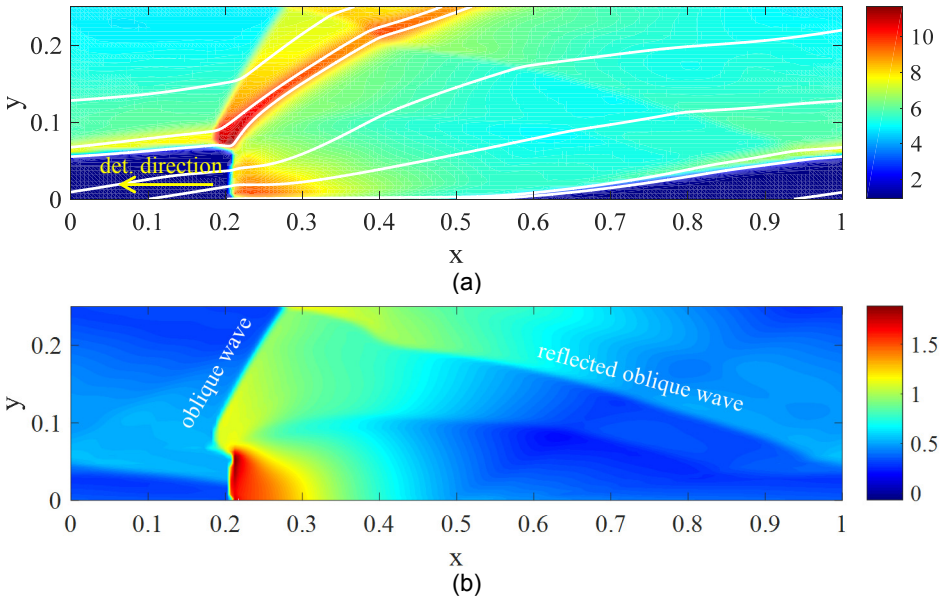


Figure 7.—Computed contours of non-dimensional temperature (a) and Log of the non-dimensional pressure (b) throughout the annulus of an RDE with $A_{exit}/A_{annulus}$ = 0.75.

both configurations are choked. As such, the flow through each (given that they are both at the same mass-averaged total temperature) is proportional to the product of the total pressure and the cross-sectional area. Using Equation (2), the entropy values listed above, and considering the post-detonation plane at x = 0.29, it can be seen that the entropy-averaged total pressure of the RDE with an exit throat is approximately 40 percent higher than the one without. However, its cross-sectional area is 25 percent less. The product of the higher total pressure and lower area indicate a 5 percent increase in mass flow rate for the RDE with a throat. This is quite close to the 2.6 percent increase observed, given the approximate nature of the analysis, and lends credence to the mechanism proposed, namely that the increase in available pressure outweighs the decrease in available area.

## A. Unstable Operation

It is tempting to further restrict the exhaust throat and see if additional gains can be made. In this idealized environment, and with this particular simulation however, it becomes difficult to do so. The reflected waves from the throat become stronger and begin to significantly affect the inflow process. Additionally, they begin to reflect from the inlet back to the throat, and then back again to the inlet, etc., until the annulus is filled with a host of spurious waves. The waves and the perturbed inflow in turn impact the detonation, which produces even more complexity in the flowfield. In the present simulation, the process is a cascading one leading to either a failure of the detonation or a non-convergent, nearly random cycle that performs poorly.

The beginnings of this cascade are illustrated in Figure 8 which shows contours of temperature at three different times after the Figure 8 exit area ratio has been reduced from $A_{exit}/A_{annulus}$ = 0.75 to 0.70. The first time represents 3 revolutions of the detonation after the abrupt area change. Each time after that represents an additional revolution. The aforementioned waves and their evolving impact are clearly seen. This is not considered a viable operational mode in this paper, so further restrictions of the exit area were not pursued.

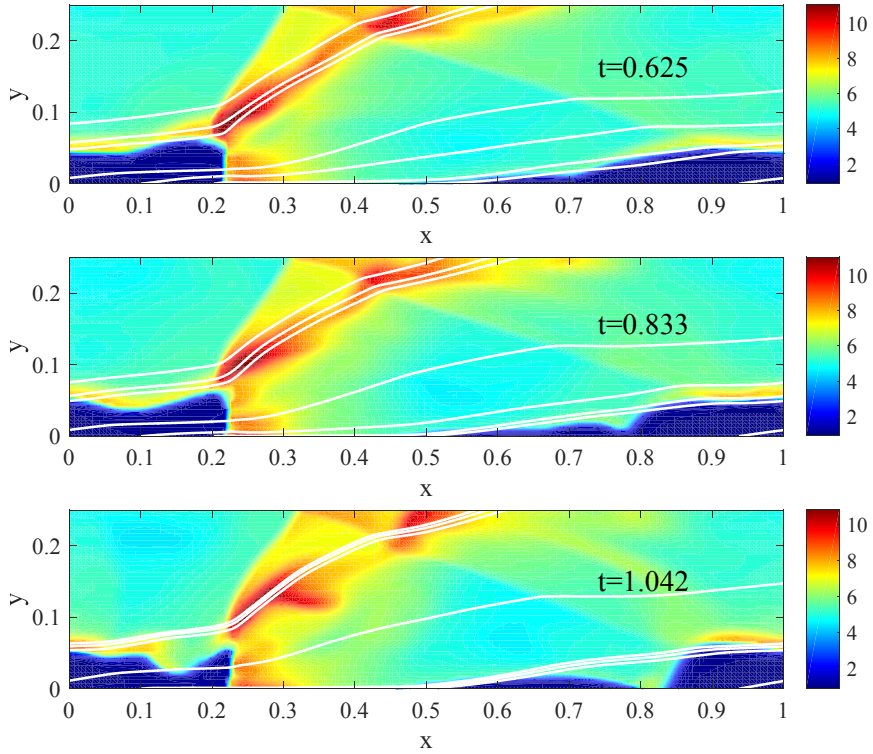


Figure 8.—Computed contours of non-dimensional temperature at successive times after the exit area has been reduced from $A_{exit}/A_{annulus}$ = 0.75 to 0.70.

Although the occurrence of this cascade is reasonable physically, it is possible that it is somehow numerically induced due to the particular formulation of the CFD model used here. Further analysis is required. It cannot be validated experimentally yet since most RDE rigs operating presently do not have anything approaching an ideal inlet. As such, they are driven by very high pressure manifolds. The inlet flows are generally under hard choke (and very high loss) and show little mass flow rate perturbation due to internally reflected waves.

## B. Stabilization Through Inlet Total Pressure Loss

Remarkably, a partial remedy to this scenario is found by introducing what may be considered a real-world loss. Specifically, the addition of a non-aerodynamic restriction at the inlet of the RDE (as is likely to exist in any practical device) (Refs. 1, 7, and 8) allows smaller exit area ratios and ultimately higher performance. This is somewhat surprising since non-aerodynamic inlet restrictions carry with them total pressure losses. However, they also seem to mitigate the effects of the waves reflected from the exit on to the inlet flow, which allows for greater exit restrictions and ultimately improved specific impulse (though flow rates are obviously reduced). By way of example a value of $A_{in}/A_{annulus} = 0.75$ was imposed at the inlet and the exit throat size was reduced until just before the unstable behavior of Figure 8 commenced. A stable simulation with $A_{exit}/A_{annulus} = 0.70$ was obtained. The temperature and pressure contours are shown in Figure 9. Comparing this figure to Figure 7 it is seen that the detonation height is reduced slightly, and the reflected oblique shock has strengthened. The entropy-averaged total pressure in the inlet plane (i.e., y = 0.0, just aft of the inlet throat) indicates a 10 percent drop relative to the manifold caused by the restriction there. Nevertheless, the benefits of the additional exit restriction outweigh this penalty, yielding an ideal net specific impulse of 4243 sec. This is a 10.3 percent improvement over the Figure 1 configuration and even a 0.8 percent improvement over the Figure 7 configuration. The mass flow rate is found to be 6 percent below the Figure 1 configuration.

The beneficial effects of the restriction arise not just from the reduction in fill Mach number, but from the now significant reflected oblique compression wave through which nearly all of the pre-detonative inflow passes (see lower left of Fig. 9(b)). The entropy-averaged total pressure just to the left of the detonation front (i.e., x = 0.19, 0<y<0.043) is an astonishing 17 percent above the inlet manifold pressure, despite the 10 percent aerodynamic loss caused by the inlet restriction. The mass-averaged Mach number at this location is 0.22; lower, as expected, than any previous configuration. The mass-averaged, post-detonative entropy at x = 0.29, 0<y<0.083 is just 7.86.

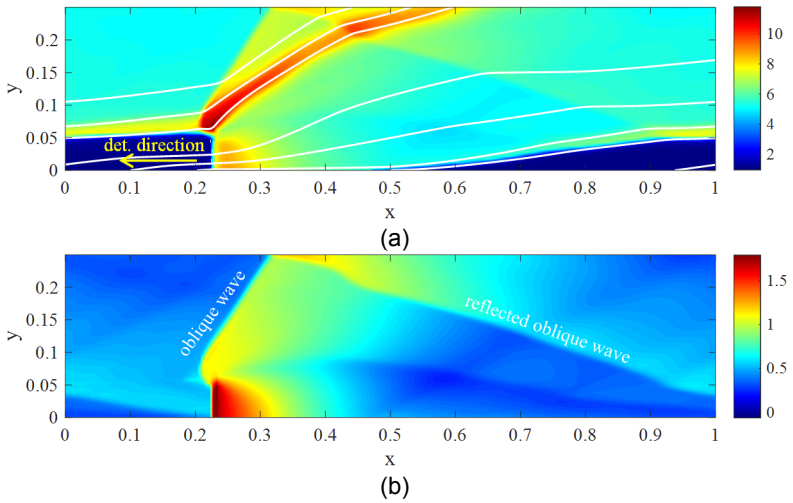


Figure 9.—Computed contours of non-dimensional temperature (a) and Log of the non-dimensional pressure (b) throughout the annulus of an RDE with $A_{exit}/A_{annulus} = 0.70$ and $A_{in}/A_{annulus} = 0.75$.

## VI. Discussion

The improvements just presented do not necessarily represent the maximum that could be obtained. It is possible that further inlet restriction could allow further exit restriction. The result presented was obtained through numerous simulations whereby the two restriction area ratios were incrementally and successively made smaller and the simulation was run to a steady-state solution. Figure 8 simply represents the respective restrictions reached at the time of this publication.

That being said, it could be argued that the value of obtaining maximum performance through maximum restriction using this highly idealized and very simplified computational approach, is dubious. The point of the present study is to demonstrate a potential pathway toward significantly improved RDE performance, and not to quantify the exact level of improvement.

Furthermore, the simulation used incorporates a notional check-valve in the RDE inlet to prevent backflow. All published RDE experiments actually utilize some type of aero-valve inlet system which attempts to minimize, but cannot prevent, backflow. The presence of an exit restriction will necessarily exacerbate any existing backflow scenario which could profoundly affect performance. The present code can approximately model this behavior (though it was not enabled for this work), and any potential future optimization/quantification efforts should include this real-world behavior.

It is also noted that RDE optimization using this approach may depend on geometrical features, namely axial length that have not yet been investigated. Examination of Figure 9(b) suggests that there may be an RDE axial length which will result in an integer number of oblique wave reflections around the circumference. This may in turn lead to a standing wave pattern (in the detonation frame of reference) whereby the perturbations to the inlet flow, while not small, are fixed. The result could be a stable operating point compared to Figure 8.

## VII. Conclusion

It has been demonstrated through an idealized, two-dimensional, computational fluid dynamic (CFD) based simulation that the basic rotating detonation engine (RDE) configuration operates with a very high average fill Mach number. This leads to lower than expected performance as measured by idealized net specific impulse. The relationship between fill Mach number and lost specific impulse has been shown to be the same for a RDE as for a pulse detonation engine (PDE) where the flowfield is predominantly one-dimensional. It has further been demonstrated that a particular approach to reducing fill Mach number, namely, an exit flow restriction or throat can improve performance by nearly 10 percent over the basic configuration. When the exit restriction becomes too severe, it is shown that a kind of unstable operation ensues. However, it is also demonstrated that the addition of a non-aerodynamic RDE inlet can add stability, and ultimately lead to specific thrust improvements in excess of 10 percent.

## References


1. Paxson, D.E., “Numerical Analysis of a Rotating Detonation Engine in the Relative Reference Frame,” AIAA-2014-0284, Jan., 2014, also NASA/TM—2014-216634, 2014.
2. “Model Specification for Engines, Aircraft, Turbojet, Military Specification MIL-E-5008B,” Department of Defense, January 1959.
3. Paxson, D.E., Kaemming, T.A., “Influence of Unsteadiness on the Analysis of Pressure Gain Combustion Devices,” *Journal of Propulsion and Power*, Vol. 30, No. 2, pp. 377-383, 2014.
4. Heiser, W.H., Pratt, D.T., “Thermodynamic Cycle Analysis of Pulse Detonation Engines,” *Journal of Propulsion and Power*, Vol. 18, No. 1, pp. 68-76, 2002.
5. Paxson, D.E., Brophy, C.M. and Bruening, G.B., “Performance Evaluation of a Pulse Detonation Combustion Based Propulsion System Using Multiple Methods,” *JANNAF Journal of Propulsion and Energetics*, Vol. 3, No. 1, May, 2010, pp 44-54.
6. Thompson, P.A., Compressible Fluid Dynamics, McGraw-Hill, 1988, pp. 347-358.

7. Paxson, D.E., Fotia, M.L., Hoke J.L., Schauer, F.R. “Comparison of Numerically Simulated and Experimentally Measured Performance of a Rotating Detonation Engine,” AIAA-2015-1101, Jan., 2015.
8. Rankin, B., Fotia, M.L., Paxson, D.E., Hoke, J.L., Schauer, F.R., “Experimental and Numerical Evaluation of Pressure Gain Combustion in a Rotating Detonation Engine,” AIAA paper 2015-0877, January, 2015.
9. Perkins, H.D., et al., “An Assessment of Pulse Detonation Engine Performance Estimation Methods Based On Experimental Results,” AIAA-2005-3831, July, 2005.
10. Paxson, D.E., Naples, A.G., Hoke, J.L., Schauer, F. “Numerical Analysis of a Pulse Detonation Cross Flow Heat Load Experiment,” AIAA-2011-584, January, 2011.
11. Paxson, D.E., Schauer, F.R., Hopper, D., “Performance Impact of Deflagration to Detonation Transition Enhancing Obstacles,” AIAA-2009-0502, July, 2009, also, NASA/TM—2012-217629.
12. Paxson, D.E., “A General Numerical Model for Wave Rotor Analysis,” NASA TM 105740, 1992.
13. Paxson, D.E., “An Improved Numerical Model for Wave Rotor Design and Analysis,” AIAA-93-0482, January, 1993.
14. Kaemming, T.A., Dyer, R.S., “The Thermodynamic and Fluid Dynamic Functions of a Pulsed Detonation Engine Nozzle,” AIAA-2004-3916, July, 2004.
15. Paxson, D.E., Kaemming, T.A., “Foundational Performance Analyses of Pressure Gain Combustion Thermodynamic Benefits for Gas Turbines,” AIAA-2012-0770, January, 2012.